Available online at www.sciencedirect.com
ScienceDirect
Thermochimica Acta 462 (2007) 32–37
thermochimica acta
www.elsevier.com/locate/tca

On the use of micro thermal analysis to characterize compatibility of nitrile rubber blends

D.K. Setua *, Y.N. Gupta

Defence Materials and Stores Research and Development Establishment, P.O. Dmsrde, G.T. Road, Kanpur 208013, India

Received 24 February 2006; received in revised form 4 June 2007; accepted 10 June 2007
Available online 20 June 2007

Abstract

The paper describes the use of micro thermal analyzer (μTA) for assessment of compatibilization in blends of nitrile rubber (NBR) with neat high-density polyethylene (HDPE), phenolic resin modified together with dynamically vulcanized HDPE and polyvinyl chloride (PVC). Micro thermal analyzer (μTA) was employed to identify different locations by the study of thermal conductivity of the surface and topographic features. Local thermal analysis (LTA), e.g., micro thermomechanical analysis (μTMA) and micro differential thermal analysis (μDTA), were conducted at these locations. Blending of NBR with unmodified HDPE shows incompatibility. Modification of HDPE by phenolic resin and dynamic cross-linking by peroxide resulted in technological compatibilization of the blend, while NBR and PVC generated characteristics of a miscible blend.

Keywords: Nitrile rubber blends; Compatibilization; Phase morphology; Atomic force microscopy; Micro thermal analysis; Local thermal analysis

1. Introduction

With the advent of micro thermal analyzer (μTA), sophisticated characterization of compatibility of elastomer blends has become a reality. Setua and White [1–4] earlier described flow visualization of mixing and phase morphology development of binary and ternary rubber blends of nitrile rubber (NBR) with other rubbers where the components had varied in level of relative polarity and solubility parameter. Scanning electron microscopy (SEM) was utilized to evaluate phase morphology of the blends. Subsequently, these studies were also extrapolated to characterize compatibility of NBR and ethylene propylene diene monomer (EPDM) rubber by many other analytical techniques, viz., Fourier transform infrared spectroscopy (FTIR), ultrasonic interferometry, atomic force microscopy (AFM) and thermal techniques, e.g., dynamic mechanical analysis (DMA), modulated differential scanning calorimetry (MDSC), thermomechanical analysis (TMA), etc. [5,6]. Attention was also focused on the estimation of efficacy of different compatibilizers, e.g., chlorinated polyethylene (CM) or chlorosulphonated polyethylene (CSM) to impart blend homogenization. Addition of a suitable compatibilizer was found to result in development of finer scale of dimension of the dispersed phase into the matrix as well as enhancement of physico-mechanical properties of the vulcanizates. Subsequently, Setua et al. [7] also reported on the preparation of thermoplastic elastomer (TPE) blends of NBR with either neat HDPE or phenolic resin modified HDPE coupled with dynamic vulcanization of the blend by peroxide. The purpose was to develop a substitute for the NBR—polyvinyl chloride (PVC) blend particularly for oil and fuel resistance applications. Wide angle X-ray scattering (WAXS) technique was adopted to determine the percentage crystallinity, i.e., the concentration of hard block in these TPEs, which govern many physico–mechanical properties.

However, a comparative assessment of the phase morphology and extent of comptabilization or interface characteristics are yet to be reported. In the present study, an attempt has been made to conduct an in depth characterization of the phase morphology of binary blends of NBR with HDPE (neat or modified version) as well as with PVC which have potential industrial applications and simultaneously explore the capability of one of the latest

* Corresponding author. Tel.: +91 512 2403202; fax: +91 512 2450404.
E-mail address: dksetua@rediffmail.com (D.K. Setua).

0040-6031/$ – see front matter © 2007 Elsevier B.V. All rights reserved.
doi:10.1016/j.tca.2007.06.004

Table 1
Characteristics of the material used

Material	Specification	Source
NBR	Grade N 533 acrylonitrile content = 33%, Mooney viscosity ML_{1+4} at 100 °C = 48	Apar Polymers Ltd., India
HDPE	MFI = 16	Polyolefin Industries Ltd., India
50:50 NBR/PVC blend	Ap-NVC 155	Apar Polymers Ltd., India
Phenolic resin	Grade-SP 1045	Hardcastle and Wand Manufacturing Co., India
Stannous chloride ($SnCl_2 \cdot 2H_2O$)	T_m = 37.7 °C	E. Merck, India
Dicumyl peroxide (DCP)	mp = 38 °C, 99.8%	Aldrich, USA
Sulfur	AR grade	BDH, India
Tetramethyl thiuram disulphide (TMTD)	Sp Gr. = 1.42, mp = 140 °C	ACCI, India
Mercaptobenzo-thiazyl sulphide (MBT)	Sp gr. = 1.54, mp = 167 °C	ACCI, India

thermal techniques (viz., μTA) for critical analysis of microstructural aspects of compatibilization.

Details of processing and molding, mechanical properties and varied applications of NBR/PVC blends, particularly in LPG tubing, automobile products and in 'O' ring and seal etc., have been reported recently [8]. Many halogen free TPEs have been evaluated as a substitute for NBR/PVC [9,10]. However, these show poor mechanical properties due to inadequate physical and chemical interactions across the boundary of the component phases resulting in a poor stress transfer.

Characterization of micro-morphology necessitates the use of a highly sophisticated and advanced analytical technique, e.g., optical microscopy, electron microscopy or analytical microscopy, viz., IR, Raman, AFM, etc. for mapping the spatial distribution of phases. None of these techniques has, however, achieved the status of desired reliability and recommended for use as standard tool owing to variety of limiting factors, e.g., resolution, specificity, difficulties in sample preparation and extended time required to acquire high resolution images [11]. On the other hand, thermal analysis methods are fast, reproducible, sensitive to small stimuli and constitute one of the most widely used techniques for such studies [12]. Conventional thermal analysis, however, fails to provide microscopic informations. The role of AFM is particularly important as it can provide three-dimensional (3D) images allowing an examination of the real particle morphology including the vertical dimension [13,14]. The 3D images can also distinguish the structurally nonequivalent particles based on their size and other morphological characteristics. The availability of micro thermal analyzer μTA 2990 developed by TA Instruments, New Castle, DE, USA which leads to the emergence of a new generation thermal analysis technique that combines the standard contact mode of AFM imaging, though at a reduced spatial resolution, with micro scale thermal analysis [15]. Description and operation principles of μTA have been reported elsewhere [16].

Measurement of thermal response of the specimen in a localized region has several advantages over a similar study on macroscopic scale. The measurement on bulk represents a result which is sum of all the constituents in the specimen. In such case, the thermal response is often dominated by higher concentration of the matrix material and, therefore, difficult to study the characteristics of the dispersed components of a blend like contaminants, additives or fillers/reinforcements, etc. Earlier studies reported on μTA were centered on the characterization of multilayer films [17], investigation of pharmaceutical matrices [18], identification of different phases in polymer blends [19], evolved gas analysis [20] and parchment [21]. Recently, few workers have reported the procedure and methodology to determine the quantitative value of the heat conductivity [22,23]. However, in these two studies the authors have reported that for reliable determination of quantitative value of thermal conductivity, the sample roughness should be approximately 20 nm (rms value). The characterization of industrial polymers using standard AFM has also been reported elsewhere [24].

2. Experimental

Details of materials and their source are listed in Table 1. Formulations of the blends are presented in Table 2. Blends of NBR and HDPE (Mixes A and B) were prepared in a Brabender Plasticoder (PLE-330) fitted with a cam type rotor by melt mixing of the polymers at 70 rpm and 150 °C. The modification of HDPE (for Mix B) was carried out in the Brabender at 70 rpm by melt mixing of 100 parts of HDPE with 2 parts of phenolic resin (SP-1045) and 0.4 parts of stannous chloride as catalyst at 150 °C. Addition of resin and stannous chloride were carried out at 1 min interval. Typical mixing cycle followed for Mixes A and B are given below,

Table 2
Formulations of the blends

Ingredients*	Mix A NBR/neat HDPE	Mix B NBR/resin treated HDPE	Mix C NBR/PVC
NBR	50	50	–
HDPE	50	–	–
Phenolic resin modified HDPE	–	50	–
50:50 NBR/PVC	–	–	100
DCP[a]	–	3	–
ZnO[b]	–	–	3.5
Stearic acid[c]	–	–	1.5
Sulfur[d]	–	–	1.5
MBT[e]	–	–	1.5
TMTD[f]	–	–	0.15

*All the ingredients (a–f) are added as parts per hundred parts of total polymer.

	Mix A	Mix B
Stage 1		
0 min	Addition of neat HDPE	Addition of resin modified HDPE
1–2 min	Addition of NBR	Addition of NBR
2 min	–	Addition of DCP
5 min	Dumped and passed through two-roll mill	Dumped and passed through two-roll mill
Stage 2		
0–2 min	Remixing of the blend	Remixing of the blend
2 min	Dumped and passed through two-roll mill	Dumped and passed through two-roll mill

0.15 × 0.15 m flat sheets were compression molded in an electrically heated Moore press at 170 °C and 10 MPa pressure for 3 min. Aluminum foils were used to reduce shrink marks on the surface. Later, the mold was plunged into cold water to restrict fluid flow and the sheet was taken out. The procedure is similar to that reported earlier [7].

In the case of blend of NBR/PVC (Mix C), the commercial master batch of Ap-PVC 155 was taken and the mixing operation was carried out on the two-roll open mill according to ASTM designation D 15–70 for 15 min at a friction ratio of 1:1.1. Vulcanization of the sheets was done at 160 °C, 4.5 MPa pressure for 10 min. Details of materials and methods of preparation along with physico-mechanical properties of various NBR/PVC blends have been reported earlier [7,8].

Test samples of 0.002 m diameter, in a plane disk form, were cut out from the molded test sheets and mounted on a metal stub using optical glue. μTA measurements were carried out using thermal probe at room temperature (30 ± 2 °C) in contact mode. The probe is a microscopically fine 5 μm diameter V shaped platinum wire. The microscope was placed on an antivibrating platform and both the thermal conductivity as well as the topography measurements were realized at 60 °C, with a resolution of 300 × 300 pixels across the area 50 μm × 50 μm. LTA experiments were conducted in the temperature range between ambient to 300 °C at a high heating rate (600 °C/min). Fast heating rate could be achieved because of the small sample size and low mass of the thermal probe. Current was passed through the probe to raise its temperature as well as that of the specimen with the simultaneous measurement of the resistance of the wire. Most of the energy of the probe was transferred to the heat capacity of the sample. During endothermic phase transition, as in these cases, an additional power was needed and the signal at this stage was compared to that of the reference, which could be realized as a micro differential thermal analysis (μDTA). Further, the probe was also separately loaded with a small force (∼20 nN) so that it could penetrate into the sample resulting in an additional analytical signal giving micro thermomechanical analysis (μTMA)

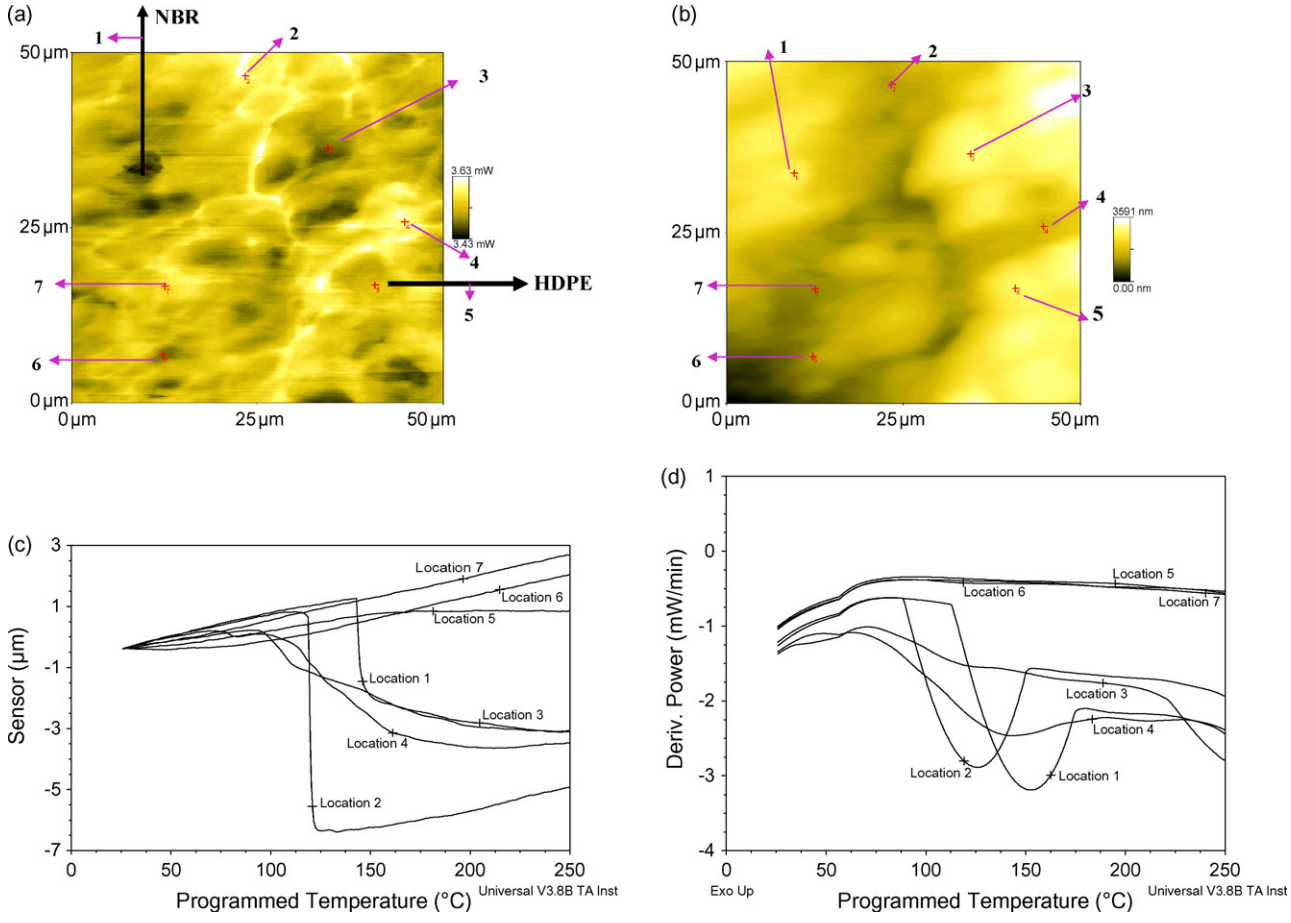

Fig. 1. (a) Thermal conductivity image of NBR and HDPE blend, (b) topography image of NBR and HDPE blend, (c) LTA (μTMA)graphs of NBR and HDPE blend and (d) LTA (DμDTA) graphs of NBR and HDPE.

data. Before performing the experiments, temperature calibration of the system was carried out using some standard samples of polyethylene terephthalate (PET) and anisic acid. Both the temperature accuracy and the reproducibility were found to be within ±2 °C.

3. Results and discussion

The thermal conductivity and corresponding topography images of NBR and pure HDPE blend (Mix A) are shown in Fig. 1(a) and (b), respectively. Brighter contrast in the thermal conductivity image of Fig. 1(a) indicates areas where more heat is dissipated from the tip of the microscopic probe, whereas the darker contrast means lesser heat dissipation. Thermal conductivity value (at 25 °C) of HDPE is 0.43 W/mK and that of NBR is 0.24 W/mK. Therefore, the areas with brighter contrast correspond to HDPE and the darker areas are due to NBR. μTA image of the blend, Fig. 1(b), presents a rough topography with formation of a variety of structures like fibril and dense segments of several inclusions of varying dimensions. These indicate generation of a grossly phase separated morphology due to immiscibility between NBR and pure HDPE. This is consistent with the proposed model for rubber-modified thermoplastics in which the rubber globules of lower conductivity are embedded by the thermoplastic matrix of higher conductivity [25].

As the probe is rastered over the sample surface artifacts may be created due to the variation in its contact area with the sample. When the probe is in a valley, it is primarily surrounded by the sample while on a peak it is surrounded by air. The movement of the probe across the sample, therefore, results in variation in heat flow depending on nature of the area of contact. Thus the black spots in the thermal conductivity image, Fig. 1(a), could be due to variations of topography of the sample surface. A limitation of the present system is that the measured conductivity depends on the area of contact and bright features in the valleys may also arise due to this.

Different locations selected for LTA are also shown in the thermal conductivity and topography images [Fig. 1(a) and (b)]. The resultant LTA graphs of μTMA and derivative micro differential thermal analysis (DμDTA) are presented in Fig. 1(c) and (d), respectively. The seven traces for locations 1–7 of LTA (for

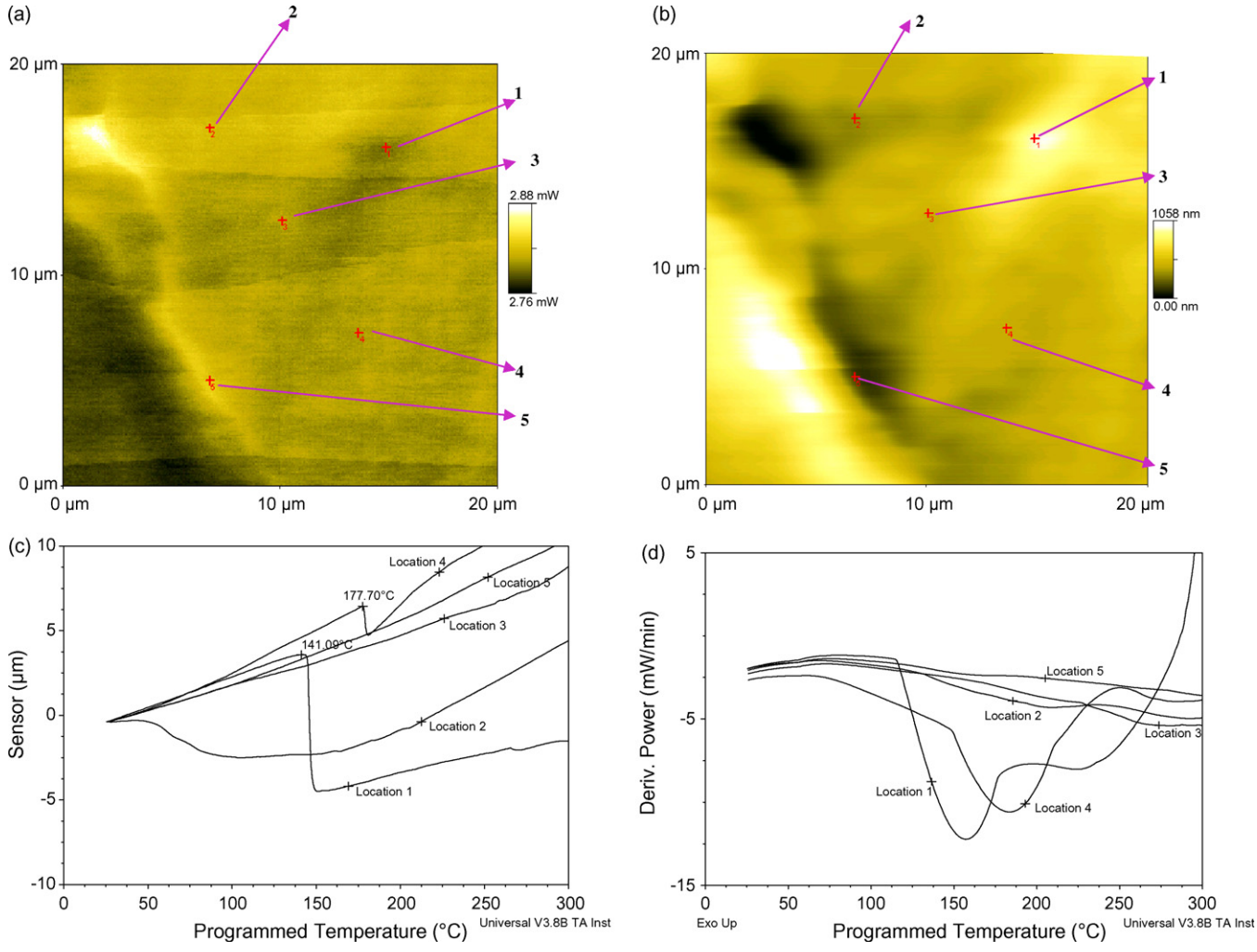

Fig. 2. (a) Thermal conductivity image of NBR and resin treated HDPE blend, (b) topography image of NBR and resin treated HDPE blend, (c) LTA (μTMA) graphs of NBR and resin treated HDPE blend and (d) LTA (DμDTA) graphs of NBR and resin treated HDPE.

either μTMA or DμDTA) reveal the presence of NBR and HDPE phases according to thermal conductivity image of Fig. 1(a). It is also apparent from Fig. 1(c) that the locations 1–4 show transitions in μTMA signal while locations 5–7 do not. These observations are also supported by DμDTA graphs [Fig. 1(d)]. Thus, curves 1–4 correspond to crystalline HDPE, while curves 5–7 correspond to amorphous NBR.

It is also apparent that the curves 3 and 4 have lower transition temperatures than curves 1 and 2. Further the magnitude of penetration of the probe in μTMA, [Fig. 1(c)], at different locations varies, with a maximum at location 2 and a minimum at location 3. LTA is a highly localized technique and variation in transition temperature at different spots is often seen due to restriction of mobility at the point of interest. It can also be mentioned that these features perhaps represent either the imperfections in HDPE or formation of a separate phase due to physical interaction between amorphous segment of HDPE with amorphous NBR. Setua et al. [7] have earlier reported the change in percentage crystallinity as measured by differential scanning calorimeter (DSC) or WAXS techniques of neat HDPE and NBR/HDPE blends. The 66% crystallinity of pure HDPE was reduced to 58% due to modification of by phenolic resin. On further blending with NBR it reduces to 28%. Elsewhere, the authors have also described the possibility of intermingling of EPDM/EPM phase with amorphous polyethylene segment of CM or CSM while compatibilization of NBR blends with EPM [1–4] or EPDM [6].

The thermal conductivity and topography images of NBR and phenolic resin treated HDPE are shown in Fig. 2(a) and (b), respectively. The different locations selected for LTA are also shown. The resultant LTA graphs for μTMA and DμDTA are presented in Fig. 2(c) and (d), respectively. In the thermal conductivity image, Fig. 2(a), varied sizes of discrete oval and elliptical shaped rubber zones of lower conductivity are found to be embedded in a continuous matrix of HDPE. Existence of separate regions of intermediate conductivity between the rubber and the matrix confirm formation of an interphase.

Sharp differences can be seen when comparing with the thermal conductivity image of NBR and neat HDPE [Fig. 1(a)] and that of NBR phenolic resin modified HDPE [Fig. 2(a)]. μTA topographic images given in Fig. 2(b) shows that the blend has lesser roughness compared to that of NBR and HDPE [Fig. 1

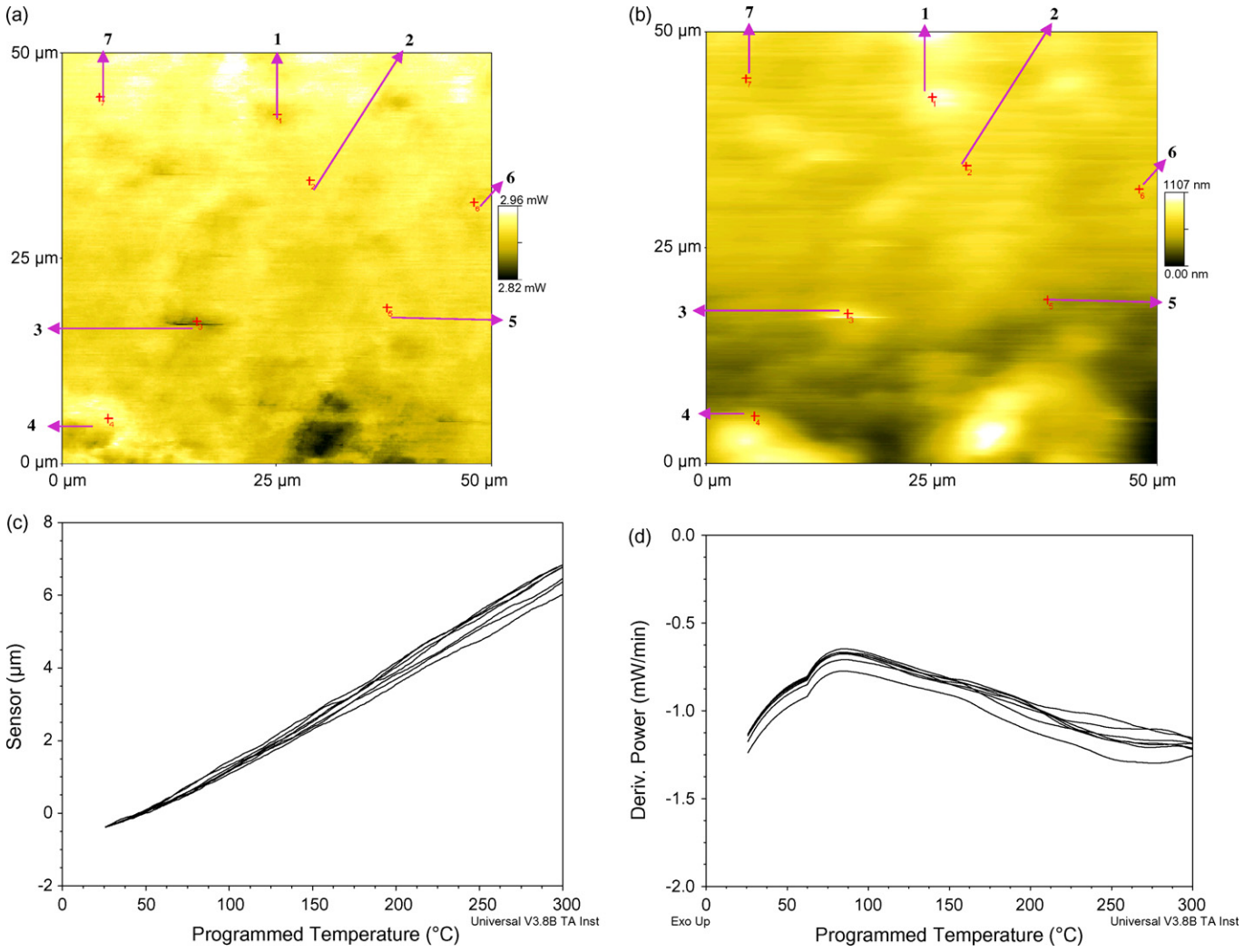

Fig. 3. (a) Thermal conductivity image of NBR and PVC blend, (b) topography image of NBR and PVC blend, (c) LTA (μTMA) graphs of NBR and PVC blend and (d) LTA (DμDTA) graphs of NBR and PVC blend.

(b)] confirming to the generation of compatibility between NBR and resin modified HDPE phases.

The LTA graphs (1–5) of μTMA presented in Fig. 2 (c) show the melting of the resin treated HDPE at locations 1 and 4 while locations 2, 3 and 5 do not show any change in the signal for the temperature range of between ambient to 250 °C. The transition temperature at location 4 is higher than location 1. This is due to the fact that at interfaces between the low conductivity rubber zone and high conductivity matrix, the mobility of phase is greatly restricted [26]. This also supports the coexistence of an interphase. These observations are also confirmed further by the DμDTA results as shown in Fig. 2(d).

It can be concluded that the locations 1 and 4 corresponds to HDPE while that of 2, 3 and 5 to NBR. However, the thermal conductivity image [Fig. 2(a)] indicates the location 1 as low conductivity spot (NBR) while location 5 as high conductivity spot due to HDPE. This is in contrary to μTMA signal of Fig. 2(c). This contradiction can be explained by the topographic image of Fig. 2 (b), where location 1 corresponds to peak while location 5 is that in a valley. Therefore, it is necessary to identify the locations of thermal conductivity image as well as topography image simultaneously. However, an accurate fingerprinting of separate spots could be done only through LTA.

The thermal conductivity and topography images of the NBR and PVC blend are presented in Fig. 3(a) and (b), respectively. It can be seen from Fig. 3(a) that the NBR/PVC blend presents a homogenous morphology with uniform contrast throughout the image. The corresponding μTA topography image, given in Fig. 3(b), also supports occurrence of a flat surface with fairly good homogeneity. The LTA (μTMA and DμDTA) plots, performed at the selected locations, are shown in Fig. 3(c) and (d), respectively. No discrete transition of any phase has been observed in the LTA experiments at selected locations of Fig. 3(a) and (b). All these support the occurrence of miscibility or formation of a homogenous phase morphology for the blend of NBR and PVC.

4. Conclusions

The capability of μTA has been explored to elucidate rubber blends and compatibility for the first time in the reported literature.

The μTA analysis of NBR and neat HDPE blend shows a phase separated morphology. Treatment of HDPE with phenolic resin and dynamic vulcanization results in an improvement of the miscibility characteristics which can be ascribed to generation of compatibility between these two phase components. Thermal conductivity and topographic images reveal that NBR and PVC is a miscible blend and no transition occurred in the LTA plots.

Micro thermomechanical (μTMA) and derivative micro differential thermal analysis (DμDTA) results reveal that artifacts may be created in the thermal conductivity image due to large topographic variations on the sample.

Further studies are needed to quantitatively estimate the values of thermal conductivity of each of the phases or additives separately in a blend as well as to measure the interfacial thickness, deformation characteristics of dispersed phase due to varied stiffness, agglomeration, grain boundary, etc.

Acknowledgement

The authors are thankful to Dr. K.U. Bhasker Rao, Director, DMSRDE, Kanpur for constant encouragement and permission to publish this work.

References

[1] D.K. Setua, J.L. White, Kautsch. Gummi Kunstst. 44 (1991) 137.
[2] D.K. Setua, J.L. White, Polym. Eng. Sci. 31 (1991) 1742.
[3] D.K. Setua, J.L. White, Kautsch. Gummi Kunstst. 44 (1991) 542.
[4] D.K. Setua, J.L. White, Kautsch. Gummi Kunstst. 44 (1991) 821.
[5] D.K. Setua, K.N. Pandey, A.K. Saxena, G.N. Mathur, J. Appl. Polym. Sci. 74 (1999) 480.
[6] K.N. Pandey, D.K. Setua, G.N. Mathur, Polym. Eng. Sci. 45 (2005) 11265.
[7] D.K. Setua, C. Soman, A.K. Bhowmick, G.N. Mathur, Polym. Engg. Sci. 1 (2002) 10.
[8] M.M. Patel, A.M. Prabhu, Paper Presented at ACS Meeting, Rubber Div., Cleveland, Ohio, Oct. 16–19, 2001 (Paper #64).
[9] S.K. De, A.K. Bhowmick (Eds.), Thermoplastic Elastomers from Rubber-Plastic Blends, Ellis Horwood Series in Polymer Science and Technology, Chicster, UK, 1990.
[10] P. Jansen, B.G. Sores, J. Appl. Polym. Sci. 84 (2002) 2335.
[11] D.M. Price, M. Reading, A. Caswell, A. Hammiche, H.M. Pollock, Microsc. Anal. 65 (1998) 17.
[12] Y.N. Gupta, A. Chakraborty, G.D. Pandey, D.K. Setua, J. Appl. Polym. Sci. 89 (2003) 2051.
[13] V. Nigam, D.K. Setua, G.N. Mathur, Rubber Chem. Technol. 73 (2000) 830.
[14] V. Nigam, D.K. Setua, Kautsch. Gummi Kunstst. 6 (2006) 316.
[15] T.R. Lever, D.M. Price, Am. Lab. Aug. 30 (1998) 15.
[16] I. Moon, R. Androsch, W. Chen, B. Wunderlich, J. Therm. Anal. Cal. 59 (2000) 187.
[17] D. Hay, H.A. Pfisterer, E.B. Storey, Rubber Age 94 (1995) 77.
[18] R.G. Royal, D.Q.M. Craig, D.M. Price, M. Reading, T.J. Lever, Int. J. Pharm. 192 (1999) 97.
[19] M. Reading, D.L. Hourston, M. Song, H.M. Pollock, A. Hammiche, Am. Lab. 30 (1998) 13.
[20] D.M. Price, M. Reading, R.M. Smith, H.M. Pollock, A. Hammiche, J. Therm. Anal. Cal. 64 (2001) 309.
[21] M. Odlyha, N.S. Cohen, G.M. Foster, A. Aliev, E. Verdonck, D. Grandy, J. Therm. Anal. Cal. 71 (2003) 939.
[22] H. Fischer, Thermochim. Acta 425 (2005) 69.
[23] S. Lefevre, S. Volz, J.B. Saulnier, C. Fuentes, N. Trannoy, Rev. Sci. Inst. 74 (2003) 2418.
[24] G.K. Barand, G.F. Meyers, MRS Bull. (2004) 464.
[25] M. Provatas, S.A. Edwards, N.R. Choudhury, Thermochim. Acta 339 (2002) 392.
[26] S.A. Edwards, M. Provatas, M.G. Markovic, N.R. Choudhury, Polymer 44 (2003) 3661.